

Chapter 11

Non-Spherical Voids: the Best Alternative to Dark Energy?

Roberto A Sussman

Abstract The constraints from current cosmological observations strongly support the Λ CDM model in which late time cosmic dynamics is dominated by a nonzero cosmological constant or by an exotic and elusive source like “dark energy”. However, these constraints can also be met if we assume a non-perturbative treatment of cosmological inhomogeneities and that our location lies within an under-dense or “void” region of at least 300 Mpc characteristic length. Since fitting observational data severely constrains our position to be very near the void center in spherical void models, we propose in this article a toy model of a less idealized non-spherical configuration that may fit this data without the limitations associated with spherical symmetry. In particular, the class of quasi-spherical Szekeres models provides sufficient degrees of freedom to describe the evolution of non-spherical inhomogeneities, including a configuration consisting of several elongated supercluster-like overdense filaments with large underdense regions between them. We summarize a recently published example of such configuration, showing that it yields a reasonable coarse-grained description of realistic observed structures. While the density distribution is not spherically symmetric, its proper volume average yields a spherical density void profile of 250 Mpc that may be further improved to agree with observations. Also, once we consider our location to lie within a non-spherical void, the definition of a “center” location becomes more nuanced, and thus the constraints placed by the fitting of observations on our position with respect to this location become less restrictive.

11.1 Introduction

Inhomogeneous cosmological models have become a valuable tool to analyze cosmological observations without introducing an elusive dark energy source (a comprehensive review on this is found in [1]). The currently preferred inhomogeneous configurations are Gpc-scale under-densities (“voids”) based on the spherically symmetric Lemaître-Tolman (LT) models [2, 3], under the assumption that we live close

R. A Sussman (✉)
Instituto de Ciencias Nucleares, UNAM, México,
Circuito Exterior C.U., 04510 México,
e-mail: sussman@nucleares.unam.mx

to a center of a cosmic density depression of radius around 1–3 Gpc [4, 5, 6]. Criticism has been voiced on these void models on the grounds that they violate the Copernican principle, since compliance with the cosmic microwave background (CMB) constraints allows for only one such Gpc structure and the observer location cannot be further away from the origin than ~ 50 Mpc [7] (see also [6]). However, as suggested by more recent work [8, 9], a void of radius 250 Mpc may be sufficient to explain the supernova observations, the power spectrum of the CMB and is also consistent with Big Bang Nucleosynthesis, or Baryon Acoustic Oscillations. By considering void structures of this size the Copernican Principle is not violated, as our Universe may consist of many such structures (the upper size to violate CMB constraints is 300 Mpc [10, 11]). Evidently, restricting our position to be within 50 Mpc from the center origin of a 250 Mpc void is a less stringent limitation. Notice that these voids are not the smaller voids (30–50 Mpc) seen in the filamentary structure of our Local Universe that roughly correspond to numerical simulations, but would form a structure a larger voids containing the smaller ones yet to be detected by observations.

In a recent article [12] we examined the possibility of using non-spherical void models to describe cosmic inhomogeneities. For this purpose, we considered the class of non-spherical Szekeres solutions of Einstein's equations [13, 14, 15, 16]. By fixing the free parameters of these solutions by means of a thin-shell approximation [10, 11, 17, 18], we obtained a specific model that yields a reasonable coarse-grained description of realistic cosmic structures. Since we define initial conditions at the last scattering surfaces, this model evolves from small early universe initial fluctuations and is consistent with current structure formation scenarios. The model presented in [12] yields an averaged spherically symmetric density distribution with a radial void profile qualitatively analogous to the spherical void models (as those of [8]), hence suggesting that the latter models may be approximate configurations that should emerge after coarse-graining and averaging of under-dense regions of a realistic lumpy non-spherical Universe. Also, the lack of spherical symmetry in the Szekeres model removes the unique invariant nature of the center location of models with this symmetry. Since our being sufficiently near this center is a strong constraint that the fitting of observations place on spherical LT models, this constraint becomes much less restrictive in a non-spherical Szekeres model.

11.2 Setting up the Szekeres Model

The metric of Szekeres models takes the following form [13]

$$ds^2 = dt^2 - \frac{(\Phi' - \Phi\mathcal{E}'/\mathcal{E})^2}{\epsilon - k} dr^2 - \frac{\Phi^2}{\mathcal{E}}(dx^2 + dy^2), \quad (11.1)$$

where $\Phi = \Phi(t, r)$ and $\Phi' = \partial\Phi/\partial r$, with:

$$\mathcal{E} = \frac{S}{2} \left[\left(\frac{x - P}{S} \right)^2 + \left(\frac{y - Q}{S} \right)^2 + \epsilon \right], \quad (11.2)$$

while $k(r), S(r), P(r), Q(r)$ are arbitrary functions; ϵ is a constant: the values $\epsilon = 1, 0, -1$ are respectively known as the quasi-spherical, quasi-plane and quasi-hyperbolic Szekeres models (for a detailed discussion on these models see [14, 15, 16]). We consider only the quasispherical case, in which the surfaces marked by r and t constant can be mapped to 2-spheres by a stereographic projection.

Einstein's equations for a dust source associated with (11.1)–(11.2) reduce to

$$\dot{\Phi}^2 = -k(r) + \frac{2M(r)}{\Phi}, \quad (11.3)$$

$$8\pi G\rho = \frac{2M' - 6M\mathcal{E}'/\mathcal{E}}{\Phi^2(\Phi' - \Phi\mathcal{E}'/\mathcal{E})}, \quad (11.4)$$

where $M(r)$ is an arbitrary function and we assume that $\Phi' \neq \Phi\mathcal{E}'/\mathcal{E}$ holds whenever $M' \neq 3M\mathcal{E}'/\mathcal{E}$, in order to avoid a shell crossing singularity [16, 26]. The solution of (11.3) is given by the quadrature

$$\int_0^\Phi \frac{d\tilde{\Phi}}{\sqrt{-k + 2M/\tilde{\Phi}}} = t - t_B(r). \quad (11.5)$$

where $t_B(r)$ marks the locus of the big bang (which is, in general, non-simultaneous). We remark that this model has no isometries (it does not admit Killing vectors), but by specializing the free functions we obtain axially and spherically symmetric models as particular cases.

By choosing the r coordinate such that $\bar{r} = \Phi(t_i, r)$, where $t = t_i$ marks the last scattering surface (and dropping the bar to simplify notation), we can eliminate one of the six independent functions of r appearing above. Thus, in order to achieve with a Szekeres model the most realistic possible description of cosmic structures and structure formation, we must prescribe five free functions as initial conditions to specify a unique model. In particular, we will specify the functions S, P, Q, t_B and M . The algorithm that we use in the calculations can be defined as follows:

1. The chosen asymptotic cosmic background is an open Friedman model¹, i.e. $\Omega_m = 0.3$ and $\Lambda = 0$. The background density is then given by

$$\rho_b = \Omega_m \times \rho_{cr} = 0.3 \times \frac{3H_0^2}{8\pi G}(1+z)^3, \quad (11.6)$$

where the Hubble constant is $H_0 = 70 \text{ km s}^{-1} \text{ Mpc}^{-1}$.

2. We choose $t_B = 0$, hence the age of the Universe (given by (11.5)) is everywhere the same (as in the homogeneous background Friedmann model) and is equal to $t_i = 471, 509.5$ years (see [20] for details).

¹ Asymptotic spatial flatness is no longer required if homogeneity is relaxed [6, 19].

3. The function $M(r)$ is given by

$$M(r) = 4\pi \frac{G}{c^2} \int_0^r \rho_b(1 + \delta\bar{\rho}) \bar{r}^2 d\bar{r},$$

where $\delta\bar{\rho} = -0.005e^{-(\ell/100)^2} + 0.0008e^{-[(\ell-50)/35]^2} + 0.0005e^{-[(\ell-115)/60]^2} + 0.0002e^{-[(\ell-140)/55]^2}$, and $\ell \equiv r/1$ kpc.

4. The function $k(r)$ can be calculated from (11.5).
5. The functions Q , P , and S are prescribed in order to provide the best possible coarse-grained description of the density distribution of our observed local Cosmography by means of a thin shell approximation (see [12]).
6. Once the model is specified, its evolution is calculated from Eq. (11.3) and the density distribution at the current instant is evaluated from (11.4).

11.3 How Realistic this Model Can be?

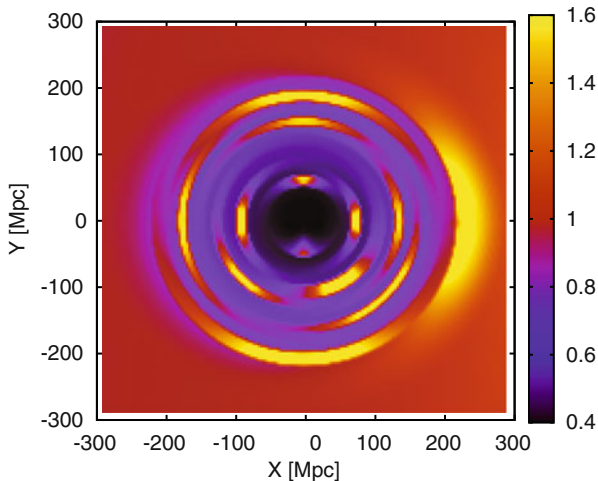
The density distribution for our model (depicted in Fig. 11.1 in intuitive Cartesian coordinates [21, 22]) follows from our choice of the functions $\{M, t_B, Q, P, S\}$. If new data would arise showing a different density pattern, we can always adjust it appropriately by selecting different functions that would change the position, size, and the amplitude of the overdensities (see [21, 22] for a detailed discussion).

As shown in Fig. 11.1, the model under consideration contains structures such as voids and elongated supercluster-like overdensities. It has large overdensities around ~ 200 Mpc (towards the left of the) that compensate the underdense regions and allow the model to be practically homogeneous at $r > 300$ Mpc. Actual observations reveal very massive matter concentrations – the Shapley Concentration roughly at the distance of 200 Mpc, or the Great Sloan Wall at the distance of 250–300 Mpc. In the opposite direction on the sky we find the Pisces–Cetus and Horologium–Reticulum, which are massive matter concentrations located at a similar distance. We refer the reader to Fig. 44 of Ref. [24], which provides a density map of the Local Universe reconstructed from the 2dF Galaxy Redshift Survey Survey using Delaunay Tessellation Field Estimator². Also, the inner void seen in Fig. 11.1 is consistent with what is observed in the Local Universe – it appears that our Local Group is not located in a very dense region of the Universe, rather it is located in a less dense region surrounded by large overdensities like the Great Attractor on one side and the Perseus–Piscis supercluster on the other side. Both are located at around 50 Mpc—see Fig. 19 of [25] that provides the density reconstruction of the Local Universe using the POTENT analysis.

While still far from a perfect “realistic” description, the density pattern displayed in Fig. 11.1 exhibits the main features of our local Universe. It should be therefore treated as a “coarse-grained” approximation to study local cosmic dynamics by means of a suitable exact solution of Einstein’s equations. Such approximation is, evidently,

² This figure is also available at <http://en.wikipedia.org/wiki/File:2dfdftfe.gif>

Fig. 11.1 The present-day color-coded density distribution ρ/ρ_0 (where ρ_0 is density of the homogeneous background model). Brighter colors indicate a high-density region, darker low-density region 11.3



far less idealized than the gross one that follows from spherically symmetric LT models.

11.4 Position of the “Center”

As a consequence of the lack of spherical symmetry, the model under consideration lacks an invariant and unique characterization of a center worldline. Instead, for every 2–sphere corresponding to a fixed value of r at an instant $t = \text{constant}$, we have (at least) two locations that can be considered appropriate generalizations of the spherically symmetric center: the worldline marked by the coordinate “origin” $r = 0$ where the shear tensor vanishes, which defines a locally isotropic observer (cf. eq (16.29) of Ref. [26]), and the “geometric” center of the 2–sphere whose surface area is $4\pi\Phi^2$.

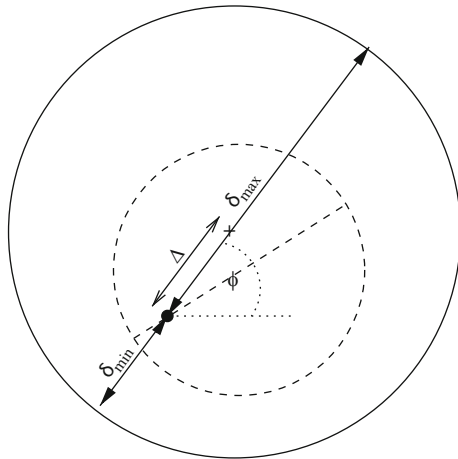
As shown in Fig. 11.2, the fact that the 2–spheres of constant r in a quasi-spherical Szekeres model are non-concentric implies that the geometric center of these spheres and $r = 0$ do not coincide. As a consequence, the distance from this origin to the surface of the sphere depends on the direction marked by the angles (θ, ϕ) of the stereographic projection (see Eq. (3) of Ref. [12]):

$$\delta(r, \theta, \phi) = \int_0^r d\tilde{r} \frac{\Phi' - \Phi\mathcal{E}'/\mathcal{E}}{\sqrt{1-k}}. \tag{11.7}$$

Hence, the displacement Δ between the origin and the geometric center of a sphere of radius r is

$$\Delta = \frac{\delta_{\max} - \delta_{\min}}{2},$$

Fig. 11.2 Schematic representation of locations that can be considered “centers” in a quasi-spherical Szekeres model: the local isotropic observer at the origin $r = 0$ (denoted by a black dot) where shear vanishes and the geometric center of the larger sphere depicted by a cross. The distance between these locations is denoted by Δ .



where $\delta_{\max} = \max(\delta)$, $\delta_{\min} = \min(\delta)$. As can be seen from Eq. (3) of [12], the maximal and minimal value of \mathcal{E}'/\mathcal{E} for our model (where $S' = 0$) corresponds to $\theta = \pi/2$. The distance, δ , as a function of ϕ for voids of various radii is depicted by Fig. 3 of [12], showing that a sphere whose present-day area radius is $\Phi = 100$ Mpc the model under consideration yields a displacement of $\Delta = 36$ Mpc towards $\phi \approx 80^\circ$ direction. While for $\Phi = 250$ Mpc we have $\Delta = 62$ Mpc towards $\phi \approx 120^\circ$.

Fitting observations in spherically symmetric models restricts our cosmic location to be within a given maximal separation from a location that is both, the geometric center of the void and the locally isotropic observer ($\Delta = 0$). It is reasonable to expect that similar distance restrictions with respect to the local isotropic observer should emerge in fitting observations with a Szekeres model, but in the latter models this observer is not the only center and may be far away from the geometric center of the void, and thus our location would be less special and improbable than in spherically symmetric models where both locations coincide.

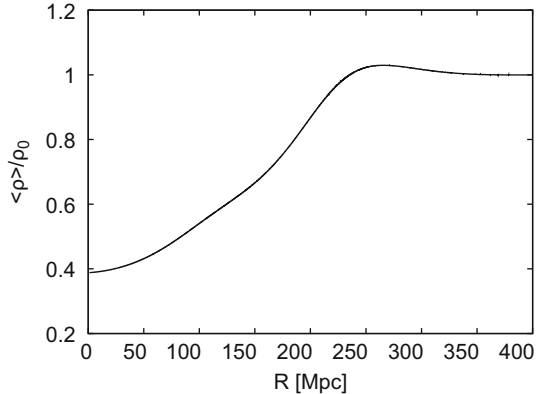
11.5 Averaging

As shown in Ref. [23], the proper 3-dimensional volume in space slices orthogonal to the 4-velocity ($t = \text{constant}$) in a Szekeres model is

$$V_{\mathcal{D}} = \int_0^{r_{\mathcal{D}}} dr \int_{-\infty}^{\infty} dx \int_{-\infty}^{\infty} dy \sqrt{-g} = 4\pi \int_0^{r_{\mathcal{D}}} dr \frac{\Phi^2 \Phi'}{\sqrt{1-k}} \equiv 4\pi R_{\mathcal{D}}, \quad (11.8)$$

and thus, the proper volume averaged density is spherically symmetric (*i.e.* independent of x and y), even if the density itself is far from a spherical distribution:

Fig. 11.3 Radial profile of the spherically symmetric averaged distribution (normalized by the background density ρ_0)



$$\begin{aligned}
 \langle \rho \rangle(r_{\mathcal{D}}) &= \frac{1}{V_{\mathcal{D}}} \int_0^{r_{\mathcal{D}}} dr \int_{-\infty}^{\infty} dx \int_{-\infty}^{\infty} \rho dy \sqrt{-g} \\
 &= \frac{1}{8\pi G R_{\mathcal{D}}} \int_0^{r_{\mathcal{D}}} dr \frac{2M'}{\sqrt{1-k}}. \tag{11.9}
 \end{aligned}$$

The radial profile of this spherical volume-averaged density distribution evaluated as a function of $r_{\mathcal{D}}$, is displayed by Fig. 11.3. The spherical symmetry of the averaged density distribution implies that the the averaging process has smoothed out the “angular” (*i.e.* x, y) dependence of a highly non-spherical coarse grained density distribution. Since the resulting averaged distribution $\langle \rho \rangle(r_{\mathcal{D}})$ is equivalent to a spherical cosmic void whose radius is approximately 250 Mpc (as in Ref. [8]), the latter type of void models can be thought of as rough averages of more realistic non-spherical configurations. As a consequence, the use of a Szekeres model seems to suggest that results obtained by means of spherical LT models may be robust: while local non-spherical information could still provide important refinements, and is needed for computations involving null geodesics (specially when fitting CMB constraints), it is likely that basic bottom line information is already contained in the spherical voids constructed with LT models.

11.6 Conclusions

The model we have presented is one among the first attempts in using the Szekeres solution as a theoretical and empiric tool to study and interpret cosmological observations [28, 29, 9, 30]. This opens new possibilities for inhomogeneous cosmologies, as this is the most general available cosmological exact inhomogeneous

and anisotropic solution of Einstein's equations. The model provides a more nuanced and much less restrictive description of the need to constrain our location with respect to a center location. It is also a concrete example that illustrates the possibility that a mildly increasing void profile (required by observations) can emerge if local structures are coarse-grained and then averaged. Of course, notwithstanding these appealing features, the model and its assumptions must be subjected to hard testing by data from the galaxy redshift surveys, and evidently the more comprehensive this data can be the better it can be used for this purpose. Unfortunately current surveys like 2dF of SDSS do not cover the whole sky and only focus on small angular regions of it. However in the near future this limitation may be overcome – for example, Sky Mapper³ aims to cover the whole southern sky which will provide sufficient data to test possibilities suggested and elaborated in this work. A more comprehensive and detailed article on the model proposed here is currently under elaboration and will be submitted soon for publication.

References

1. K. Bolejko et al., *Structures in the Universe by Exact Methods—Formation, Evolution, Interactions*, Cambridge University Press, Cambridge, 2009
2. G. Lemaître, *Ann. Soc. Sci. Bruxelles A53* (1933) **51**; English translation, with historical comments: *Gen. Rel. Grav.* **29** 637 (1997)
3. R.C. Tolman, *Proc. Nat. Acad. Sci. USA* **20** (1934) 169; reprinted, with historical comments: *Gen. Rel. Grav.* **29** 931 (1997)
4. H. Alnes, M. Amarzguioui, O. Gron, *Phys. Rev.*, **D73** 08351 (2006)
5. J. García-Bellido, T. Haugbolle, *J. Cosmol. Astropart. Phys.* **04** 003 (2008)
6. K. Bolejko and J. S. B. Wyithe, *J. Cosmol. Astropart. Phys.* **02** (2009) 020.
7. H. Alnes, M. Amarzguioui *Phys. Rev. D* **75** 023506 (2007)
8. H. Alnes, M. Amarzguioui, *Phys. Rev. D* **75** (2007) 023506.
9. K. Bolejko and M.-N. Célérier, *Phys. Rev. D* **82** 103510 (2010)
10. K.T. Inoue and J. Silk, *Astrophys. J.* **648** 23 (2006)
11. K.T. Inoue and J. Silk, *Astrophys. J.* **664** 650 (2007)
12. K. Bolejko and R.A. Sussman, *Phys Lett B* **697** 265–270
13. P. Szekeres, *Commun. Math. Phys.* **41** 55 (1975)
14. C. Hellaby, A. Krasinski, *Phys. Rev. D* **77** 023529 (2008)
15. A. Krasinski *Phys. Rev. D* **78** 064038 (2008)
16. C. Hellaby, A. Krasinski, *Phys. Rev. D* **66** 084011 (2002)
17. K.L. Thompson and E.T. Vishniac, *Astrophys. J.* **313** 517 (1987)
18. K. Tomita, *Astrophys. J.* **529** 38 (2000)
19. C. Clarkson, M. Regis, arXiv:1007.3443 (2010)
20. P.J.E. Peebles, *The Large-Scale Structure of the Universe*. Princeton University Press, Princeton (1980)
21. K. Bolejko, *Phys. Rev. D* **73** 123508 (2006)
22. K. Bolejko, *Phys. Rev. D* **75** 043508 (2007)
23. K. Bolejko, *Gen. Rel. Grav.* **41** 1585 (2009)
24. R. van de Weygaert and W. Schaap in *Data Analysis in Cosmology*, ed. V. Martínez, E. Saar, E. Martínez-González, M. Pons-Bordería, Springer-Verlag, Berlin, *Lecture Notes in Physics* **665** p. 291 (2009)

³ <http://msowww.anu.edu.au/skymapper/>

25. A. Dekel, et al., *Astrophys. J.* **522** 1 (1999)
26. J. Plebański, A. Krasinski, *An introduction to general relativity and cosmology*. Cambridge University Press, Cambridge (2006)
27. T. Buchert, *Gen. Rel. Grav.* **40** 467 (2008); R. Zalaletdinov, *Int. J. Mod. Phys. A* **23** 1173 (2008)
28. M. Ishak, J. Richardson, D. Garred, D. Whittington, A. Nwankwo, R. Sussman, *Phys. Rev. D* **78** 123531 (2008)
29. A. Nwankwo, J. Thompson, M. Ishak, arXiv1005.2989 (2010)
30. A. Krasinski, K. Bolejko, arXiv:1007.2083 (2010)